Algorithms for ocean bottom albedo determination from in-water natural light measurements

Robert A. Leathers

Earth System Science Office, NASA, Code SA00, Stennis Space Center, Mississippi 39529

Norman J. McCormick

Department of Mechanical Engineering, University of Washington, Box 352600, Seattle, Washington 98195-2600

Abstract

A method for determining the ocean bottom optical albedo, R_b, from in-water upward and downward irradiance measurements at a shallow site is presented, tested, and compared with a more familiar approach that requires additional measurements at a nearby deep-water site. Also presented are two new algorithms for the estimation of R_b from measurements of the downward irradiance and vertically upward radiance. All methods performed well in numerical situations at depths where the influence of the bottom on the light field was significant.

Keywords: ocean optics, radiative transfer, inverse problem, bottom albedo

OCIS codes: 010.4450, 030.5620, 100.3190, 999.9999

1. Introduction

For shallow ocean waters, knowledge of the optical bottom albedo, R_b, is required to model the underwater[1,2] and above-water[3] light field, to enhance underwater object detection or imaging,[8] and to correct for bottom effects in the optical remote sensing of water depth[4,5] or inherent optical properties (IOP's).[6,7] Measurements of R_b can also help one identify the bottom sediment composition,[5] determine the distribution of benthic algal or coral communities,[9] and detect objects embedded in the seafloor. Furthermore, values of R_b, defined as the upward irradiance emerging from the bottom divided by the downward irradiance into the bottom, can be used as an integral test for attempted measurements of the bottom bidirectional reflectance function.

Although the value of the irradiance ratio, $R(z)$, equals R_b at the bottom, it is not possible to measure $R(z)$ right at the bottom, and irradiance measurements just above the bottom are difficult to obtain because of instrument self-shadow. An estimate of R_b can be made by extrapolating to the bottom measurements of $R(z)$ at several depths z near the bottom; however, extrapolation is generally unreliable because profiles of $R(z)$ typically vary sharply with depth close to the bottom.[10] *In vitro* R_b measurements of small bottom samples can be obtained with the method in Ref. 4 or of larger bottom samples with a spectral radiometer; however, these are time-consuming processes, the *in vitro* value of R_b is not necessarily equal to the *in situ* value, and it is not clear how representative these samples are of larger spatial regions of interest.

Because *in situ* estimates of R_b from light measurements close to the bottom are subject to small-scale horizontal variability of the bottom, it may be preferable to determine R_b from measurements further from the bottom, thereby obtaining horizontally-averaged values that are more appropriate for remote sensing applications and one-dimensional radiative transfer modeling. An estimate of R_b can be made[9] from a $R(z)$ measurement just below the sea surface, $R(0^+)$, together with simultaneous measurements in nearby deep water of $R(0^+)$

and the downward diffuse attenuation coefficient. Similarly, a qualitative algorithm has been proposed[5] and tested[11,12] for bottom characterization from remote radiance measurements at two wavelength bands simultaneously over both shallow and deep water. Both of these methods have the disadvantage, however, that they require that a deep-water site exists nearby that has the same water composition, illumination, and surface conditions as the shallow-water site.

A new method of solving the inverse radiative transfer problem for the determination of R_b is proposed in Sec. 2. Required are measurements of the upward and downward irradiances at one wavelength and at least two mid-water-column depths at only one site. Also proposed are two related algorithms for the estimation of R_b from measurements of the vertically upward radiance and downward irradiance. These algorithms, like the previously developed ones, require knowledge of the measurement distances above the bottom. Results of specific numerical tests for all the R_b estimation algorithms are presented in Sec. 3, and a discussion is given in Sec. 4.

2. Theory

A. Preliminaries

We are interested in the azimuthally averaged radiance $L(z,\mu)$ that satisfies the integro-differential radiative transfer equation

$$\left(\mu\frac{\partial}{\partial z}+c\right)L(z,\mu)=b\int_{-1}^{1}\tilde{\beta}(z,\mu,\mu')\,L(z,\mu')\,d\mu', \tag{1}$$

where b and c are the scattering and beam attenuation coefficients, $\tilde{\beta}$ is the azimuthally integrated scattering phase function, and μ is the direction cosine with respect to the downward depth z. All quantities in Eq. (1) implicitly depend on wavelength. The downward and upward irradiances are given by

$$E_d(z) = 2\pi \int_0^1 \mu L(z,\mu) d\mu \qquad \text{and} \qquad E_u(z) = 2\pi \int_{-1}^0 |\mu|\, L(z,\mu) d\mu. \tag{2}$$

The irradiance ratio is

$$R(z) = E_u(z)/E_d(z), \tag{3}$$

and $R(z_b) = R_b$ for water depth z_b. The analogous radiance-irradiance ratio is

$$R^L(z) = \pi L_u(z)/E_d(z), \tag{4}$$

where the vertically upward radiance $L_u(z) = L(z,-1)$. The factor π is included in the definition of $R^L(z)$ so that $R^L(z_b) \approx R_b$, with $R^L(z_b) = R_b$ for a Lambertian bottom.

With increasing depth in optically deep, spatially uniform, source-free waters, $R(z)$, $R^L(z)$, and the downward diffuse attenuation coefficient,

$$K_d(z) = -\frac{1}{E_d(z)} \frac{dE_d(z)}{dz}, \tag{5}$$

asymptotically approach values R_∞, R^L_∞, and K_∞, respectively. These asymptotic values are IOP's of the water that can be uniquely computed from b, c, and $\tilde{\beta}$.[13]

B. Irradiance ratio approach

A well known model for the irradiance ratio is[4,5,14]

$$R(z) = R_{2nd}(z) + [R_b - R_{2nd}(z)] \exp[-2(z_b - z)K_{2nd}], \tag{6}$$

where the water depth at the shallow site of interest is assumed to be known and the subscript $2nd$ denotes measurements taken at a nearby deep-water site characterized by the same illumination, sea surface conditions, and water IOP's as the site of interest. In the derivation of Eq. (6), K is taken to be $K(z) = [K_d(z) + \kappa(z)]/2$ averaged over depth in a non-specified manner, where κ is the coefficient of attenuation in the upward direction of upwelling photons[14,15] (from both in-water scattering and the bottom); a qualitative

and quantitative study of κ is given in Refs. 4 and 15. In practice, however, the value of K_{2nd} is typically approximated by the vertically averaged $K_d(z)$ at the deep-water site.[4] A rearrangement of Eq. (6) gives the algorithm evaluated by Maritorena *et al.*[4] for determining R_b from irradiance measurements at two sites,[9,16]

$$R_b = R_{2nd}(z) + [R(z) - R_{2nd}(z)] \exp[2(z_b - z)K_{2nd}]. \tag{7}$$

Equation (7) is often written for $z = 0^+$ in hope of applying it to remote sensing applications; however, it is valid for any depth, z, and is more accurate at mid-water depths than at the surface. A difficulty with implementing Eq. (7) is that a deep-water ($2nd$) site may not be available that matches the water, surface, and illumination conditions of the shallow-water site.

An alternative shallow-water model was previously derived[17] from the radiative transfer equation with the eigenfunction expansion method. In this derivation the light field is approximated by the sum of two eigenmodes that decrease in magnitude with distance away from the surface and bottom, respectively. Expressed in the form of Eq. (7), this model is

$$R_b = R_\infty + [R(z) - R_\infty] \exp[2(z_b - z)K_\infty], \tag{8}$$

which can be used to estimate R_b from measurements at a single site provided that z_b is known and R_∞ and K_∞ can be determined. It is important to note that the asymptotic in-water irradiance ratio R_∞ in Eq. (8) does not represent the same quantity denoted by that symbol in Refs. 4 and 9, where R_∞ is our $R_{2nd}(0^+)$. Equations (7) and (8) were derived with entirely independent approaches; however, their final forms are very similar, and the two theoretically converge when R_{2nd} and K_{2nd} are measured at large depths in homogenous, source-free waters, where $R_{2nd}(z) = R_\infty$ and $K_{2nd}(z) = K_\infty$.

Equation (8) provides a new interpretation of the attenuation coefficient in Eq. (7). The derivation of Eq. (7) suggests that $K \approx (K_d + \kappa)/2$, whereas the derivation of Eq. (8) suggests that $K \approx K_\infty$. Because $\kappa > K_d$,[4,15] and therefore $K > K_d$, there is a question

about the appropriateness of taking K to be the vertically-averaged $K_d(z)$. Because typically $\kappa > K_\infty > K_d$, it follows that $K = [K_d(z) + \kappa(z)]_{2nd}/2 \approx K_\infty$. Therefore, Eq. (7) may be best implemented by taking K equal to the value of $K_d(z)$ deep in the euphotic zone, where $K_d(z) \approx K_\infty$, rather than as earlier proposed.[9,16] This hypothesis is further addressed in Sec. 3.

If R_∞ and K_∞ can be determined at the shallow site of interest, then the method of Eq. (8) has the distinct advantage over that of Eq. (7) that measurements are required from only the one site. One way to determine R_∞ and K_∞ is to calculate them with the procedure in Ref. 17 from measurements of b and c obtained, for example, from water samples[18] or with a Wetlabs ac-9 instrument[19]. Alternatively, it is possible to estimate R_∞ and K_∞ from the same irradiance profile measurements (at the shallow-water site) used to form $R(z)$ without any direct measurement of the water properties. The value of R_∞ can be obtained with an equation derived[17] from a shallow-water asymptotic approximation of the light field,

$$\left[\frac{1-R_\infty}{1+R_\infty}\right]^2 = \frac{[E_d(z)-E_u(z)]^2|_{z_1}^{z_2}}{[E_d(z)+E_u(z)]^2|_{z_1}^{z_2}} \,. \tag{9}$$

To employ Eq. (9), one must subtract and add $E_u(z)$ and $E_d(z)$ at two depths, z_1 and z_2, square the results, and evaluate the differences between the two depths. Because these operations are susceptible to noise, it is important that the irradiance measurements be of high quality and their temporal variations be averaged out. The value of K_∞ in Eq. (8) can be estimated as the maximum value attained by $K_d(z)$. Because the value of $K_d(z)$ is relatively insensitive to R_b,[1] the value of $\max[K_d(z)]$ is typically approximately equal to K_∞.

C. Radiance-irradiance ratio approach

If $L_u(z)$ measurements are available rather than $E_u(z)$, then R_b can be estimated from $R^L(z)$ of Eq. (4) with a new model (derived in Appendix A), analogous to Eq. (8),

$$R_b = R^L_\infty + [R^L(z) - R^L_\infty] \exp[2(z_b - z)K_\infty]. \tag{10}$$

However, because an equation analogous to Eq. (9) has not been derived for R^L_∞, implementation of Eq. (10) requires that the value of R^L_∞ either be calculated[13] from local measurements of the IOP's or measured in nearby deep water.

We found with numerical simulations that reasonable estimates of R_b can alternatively be obtained from $R^L(z)$ with

$$R_b = R^L_{2nd}(z) + [R^L(z) - R^L_{2nd}(z)] \exp[2(z_b - z)K_{2nd}], \tag{11}$$

although we have no analytical justification for Eq. (11) other than its analogy to Eq. (7). As with Eq. (7), use of this equation requires measurements at a second (deep-water) site.

3. Numerical tests

A. Methods

Numerical tests were performed to evaluate the accuracies of Eqs. (7)–(11) for the determination of R_b. Simulated $E_u(z)$, $E_d(z)$, and $L_u(z)$ values were generated at 0.25 optical depth spacing using the discrete ordinates radiative transfer code `DISORT`.[20] The surface illumination was modeled as a combination of direct collimated sunlight and diffuse skylight. The water was defined to have locally homogenous optical properties, a relative index of refraction of 1.34 with respect to air, and scattering determined by the Petzold particle scattering phase function.[21] Spatially-dependent internal sources, such as from fluorescence, Raman scattering, or bioluminescence, were neglected. A Lambertian bottom was assumed, which provides a good approximation to the more general, but usually poorly known, bidirectional reflectance function.[1,2] Simulations were performed for various values of single scattering albedo ($\omega_0 = b/c$), R_b, percent direct sunlight, and water optical depth ($\tau_b = cz_b$). The values of R_b were taken to be in the range $0 \leq R_b \leq 0.4$, which is consistent with observations

in natural waters.[1]

Equation (8) was applied to shallow-water simulations of $E_u(z)$ and $E_d(z)$ to determine bottom albedo estimates, $\widehat{R_b}(z)$, as a function of the depth of the corresponding irradiance measurements. The values of R_∞ and K_∞ used in Eq. (8) were obtained in two different ways. First, R_∞ was determined with Eq. (9) and K_∞ was estimated from either $K_\infty(z) \approx K_d(z)$ or $K_\infty \approx \max[K_d(z)]$. Second, the IOP's of the water were assumed to be known from *in situ* measurements, and these were used to calculate R_∞ and K_∞. For comparison, $\widehat{R_b}(z)$ was also determined from $E_u(z)$ and $E_d(z)$ with Eq. (7) for combinations of shallow and deep-water simulations. Here, K was taken to be, alternatively, $K_d(z)$, $\overline{K_d(z)}$ (the vertical average of $K_d(z)$ between the surface and the depth of the shallow-water site), and K_∞ [determined from a deep (asymptotic) value of $K_d(z)$].

The bottom albedo was also determined from simulations of $L_u(z)$ and $E_d(z)$. Equation (10) was used to calculate $\widehat{R_b}(z)$ from data at only the shallow water site. The values of R_∞^L and K_∞ were calculated from the known water optical properties. In addition, $\widehat{R_b}(z)$ was determined from $L_u(z)$ and $E_d(z)$ with Eq. (11) for combinations of shallow and deep-water sites. The value of K_{2nd} was determined in the same manner as for the E_u–E_d approach.

B. Results

For all the shallow-water simulations performed, estimates of R_b obtained with Eqs. (8) and (9) approached the correct value in a nearly linear fashion within the bottom few optical depths of the water column. Extrapolation of $\widehat{R_b}(z)$ at two and one optical depths above the bottom consistently produced estimates of R_b that were accurate to within about 1%. Given in Table 1 are example $\widehat{R_b}(z)$ at three, two, and one optical depths above the bottom, as well as the linear extrapolation of the latter two to the bottom. For Table 1, the illumination conditions of the simulations were taken to be either overcast (100% diffuse) or sunny (75% direct sunlight from a zenith angle of 30°), and in the solutions for R_b the

values of K_∞ in Eq. (8) were approximated by $\max[K_d(z)]$. At a given measurement depth, estimates generally improved with increasing value of ω_0. For example, for $R_b = 0.2$, $\tau_b = 5$, and sunny skies, the error at 3 optical depths above the bottom was 15% for $\omega_0 = 0.7$ but only 3.5% for $\omega_0 = 0.9$. The value of R_b had a small effect on the accuracy of its estimate; for large ω_0 and small R_b, $\widehat{R_b}(z)$ was greater than R_b, whereas for small values of ω_0 or for a combination of large ω_0 and large R_b, $\widehat{R_b}(z)$ was less than R_b. Estimates were more accurate, but insignificantly so, with overcast conditions. Also, the depth of the water had very little effect on the accuracy of $\widehat{R_b}(z)$ at a given depth above the bottom; however, in practice, instrument noise will be more significant in relatively deep water than in very shallow water.

In most cases, estimates of R_b with Eqs. (8) and (9) were more accurate if K_∞ in Eq. (8) was approximated by $\max[K_d(z)]$ than if it was replaced by $K_d(z)$. This is because large values of K_∞ in Eq. (8) lead to large values of $\widehat{R_b}$, and the estimates of R_b were typically less than the correct value. For cases where the value of ω_0 was high and the value of R_b small, the use of $K_d(z)$ gave slightly, but insignificantly, better results than the use of $\max[K_d(z)]$.

Because Eq. (9) provides only an asymptotic approximation to R_∞, it was expected that estimates of R_b would improve if more accurate values of R_∞, calculated from the assumed known water IOP's, were used in Eq. (8). However, the numerical tests showed the reverse to be true; errors in $\widehat{R_b}$ introduced by the approximation of Eq. (9) helped counteract errors in $\widehat{R_b}$ due to the assumptions inherent in Eq. (8). Although Eq. (8) with calculated R_∞ performed similarly in the bottom half of the water column to Eq. (8) with R_∞ from Eq. (9), Eq. (8) with calculated R_∞ performed poorly in the top half of the water column and even near the bottom slightly underperformed Eqs. (8)–(9).

For example, shown in Fig. 1 are the estimates of R_b as a function of measurement optical depth obtained from simulated $E_u(z)$ and $E_d(z)$ with three different methods: from $\widehat{R_b}(z) = R(z)$, from Eq. (8) with calculated R_∞ and K_∞, and from Eqs. (8) and (9) with K_∞ replaced by $\max[K_d(z)]$. In this simulation, $R_b = 0.2$, $\tau_b = 5$, and $\omega_0 = 0.8$, and the sea

surface illumination was taken to be sunny (as defined above). Since $R_b = R(z \rightarrow z_b)$, the first approach for determining R_b is the most straightforward. This gave a smooth profile of $\widehat{R_b}(\tau)$ that monotonically approached R_b with increasing depth; however, this estimate is extremely inaccurate except very close to the bottom, with 41% error at only one optical depth above the bottom and 61% error at two optical depths above the bottom. This sharp increase in $R(z)$ near the bottom is typical[10] and makes extrapolation of $R(z)$ from mid-water depths to the bottom impractical. At all depths off the bottom, far better estimates of R_b were obtained with Eq. (8) with R_∞ and K_∞ calculated from the known water IOP's. The errors at two and one optical depths off the bottom were 11% and 5.8%, respectively. Even better estimates of R_b at all depths off the bottom, however, were obtained from Eq. (8) with R_∞ determined with Eq. (9) and K_∞ estimated by $\max[K_d(z)]$. This gave an error at two and one optical depths off the bottom of 6.2% and 2.8%, respectively. Again, extrapolation from mid-depths gave an excellent estimate of R_b.

Values of the bottom albedo from irradiance measurements at a combination of shallow and deep-water sites with Eq. (7) were consistently underestimates. Therefore, since K_∞ was generally larger than $K_d(z)$, results were more accurate when the value of K in Eq. (7) was determined from a deep value of $K_d(z)$ in the deep-water site, where $K_d(z) \approx K_\infty$, than when it was determined from either the deep-water $K_d(z)$ or $\overline{K_d(z)}$. For example, shown in Fig. 2 are $\widehat{R_b}(\tau)$ calculated from Eq. (7) with K replaced by $K_d(z)$ and by K_∞ [determined from $K_d(\tau = 15)$] for two sunny sky simulations: 1) $\omega_0 = 0.7$, $\tau_b = 5$, and $R_b = 0.1$, and 2) $\omega_0 = 0.9$, $\tau_b = 5$, and $R_b = 0.2$.

Shown in Fig. 3 are comparisons of $\widehat{R_b}(\tau)$ obtained from $E_u(z)$ and $E_d(z)$ measurements at only the shallow water site [Eqs. (8) and (9)] and $\widehat{R_b}(\tau)$ obtained from measurements at both shallow and deep water sites [Eq. (7)]. The two cases shown are sunny sky simulations with $\tau_b = 5$ and 1) $\omega_0 = 0.9$ and $R_b = 0.1$, and 2) $\omega_0 = 0.8$ and $R_b = 0.2$. As these examples demonstrate, the two-site method was typically far more accurate than the one-site method

near the surface, whereas the one-site algorithm usually outperformed the two-site method near the bottom.

Example $\widehat{R_b}(\tau)$ obtained from $L_u(z)$ and $E_d(z)$ are shown in Fig. 4 for 1) $\omega_0 = 0.9$, $R_b = 0.1$, and sunny conditions, and 2) $\omega_0 = 0.9$, $R_b = 0.2$, and overcast conditions. Because estimates of R_b with Eq. (11) were typically larger than the actual value, the $\widehat{R_b}(\tau)$ in Fig. 4 obtained with Eq. (11) were calculated with $\overline{K_d(z)}$ rather than the asymptotic K_d in order to make the estimated values as good as possible. In general, the value of ω_0 had a large impact on the accuracy of both L_u-E_d methods, with the best estimates obtained when ω_0 was large. The illumination conditions were also very important for the L_u-E_d methods, with the best results being obtained for overcast conditions. The value of R_b, on the other hand, had no significant effect on the accuracy of its estimate. Under sunny conditions, the one-site method of Eq. (10) and the two-site method of Eq. (11) performed similarly in the bottom one optical depth when ω_0 was small and in the bottom three optical depths when ω_0 was large, but Eq. (11) was considerably more accurate than Eq. (10) near the surface. For overcast conditions, Eq. (10) performed well at all depths but still underperformed Eq. (11).

4. Discussion

Several methods were evaluated here for the determination of R_b from common natural light measurements. Each method returns accurate values of R_b if implemented very close to the bottom. However, because it is difficult in practice to obtain light field measurements very close to the bottom, it is necessary to apply these algorithms at one or more optical depths off the bottom and, when possible, extrapolate the depth-dependent estimates to the bottom. Therefore, it is desirable that the error of the method used is both small and linearly decreasing with depth. The methods were all found to be preferable to a straightforward extrapolation of $R(z)$ to the bottom, where $R(z) = R_b$, but differed in their accuracies when applied more than one or two optical depths away the bottom.

Estimates of R_b can be obtained with Eq. (8) by first estimating R_∞, either with Eq. (9) or by calculating it from known water IOP's. This method does not require measurements at other wavelengths or at another site, and estimates of R_b from this method at one or two optical depths off the bottom were generally found to be more accurate than those obtained with Eq. (7). Numerical simulations indicated that the use of R_∞ from Eq. (9) produces better estimates of R_b than the use of the value of R_∞ computed from the IOP's. This is because, fortuitously, the error introduced into Eq. (8) by applying it where the light field is not well described by the assumed two-mode asymptotic model (see Appendix) is mitigated by the deviation in the value of R_∞ predicted by Eq. (9) from its true value. Therefore, even if the water IOP's are known, it is preferable to employ Eq. (9), provided the processed data has a relatively smooth $\widehat{R_b}(\tau)$ profile. Unfortunately, this method is often inaccurate near the sea surface when the bottom signal is not strong.

If one wishes to estimate R_b from measurements close to the surface and a suitable deep-water site is available, then Eq. (7) provides the most reliable method. However, it was found that if the deep water site is vertically well mixed, then Eq. (7) should be implemented by replacing K_{2nd} with K_∞, which can be directly measured deep in the euphotic zone of the deep water site.

Estimates of R_b alternatively can be made from measurements of $L_u(z)$ and $E_d(z)$ with Eq. (10), provided that the bottom is approximately Lambertian. Equation (10) requires that R_∞^L either be analytically computed from local measurements of the water IOP's or measured at a nearby deep-water site. If a suitable second site is readily available, Eq. (11) should be used instead since it was found to be generally more accurate and reliable than Eq. (10). However, both L_u-E_d methods performed well when applied in the bottom half of the water column. The inaccuracy of Eq. (10) under sunny conditions makes it unsuitable for remote sensing applications, and therefore Eq. (10) offers no advantage over the E_u-E_d method (which is the more natural approach to *in situ* R_b estimation). Equation (11), on

the other hand, shows some promise for remote sensing applications for large ω_0 (or for any ω_0 if ω_0 is known).

Regardless of the method used, the determination of R_b is easiest when the bottom signal is strong. Thus, R_b can be obtained most accurately when the water is shallow, the value of R_b is large, and the attenuation of the water is low (e.g., over tropical coral reefs or white sandy beaches). If the bottom composition is believed to be uniform over a large horizontal region, then the determination of R_b should be made at the shallowest depth.

In practice, the method to use for the estimation of R_b will be dictated by the instrumentation available and whether or not an appropriate deep-water site exists. Given the choice, however, the estimation of R_b should be done with measurements of $E_u(z)$ rather than with $L_u(z)$. The most informative approach would be to use all the methods discussed here and intercompare the results. If the estimates agree they can be recorded with great confidence. On the other hand, the difference between estimated R_b values from $R(z)$ and $R^L(z)$ might serve as a crude measure of the degree to which the bottom behaves as a Lambertian surface. However, for purposes of modeling the light field, Mobley[22] has demonstrated that it is far more important to measure the magnitude of the effective bottom albedo than it is to obtain the detailed angular pattern of the bottom bidirectional reflectance function.

ACKNOWLEDGMENTS

This research was supported by the U. S. Office of Naval Research. The radiative transfer numerical code DISORT was kindly provided by Knut Stamnes.

Appendix A: Derivation of Eq. (10)

If the optical properties of the water are spatially uniform and there are no internal sources, then when cz is at least one optical depth away from a boundary the upward radiance and

downward irradiance can be expressed as summations of eigenmodes,[13]

$$L_u(z) = L(z,-1) = \sum_{j=1}^{J} [C(\nu_j)\phi(\nu_j,-1)\exp(-cz/\nu_j) + C(-\nu_j)\phi(-\nu_j,-1)\exp(cz/\nu_j)], \quad \text{(A1)}$$

$$E_d(z) = \sum_{j=1}^{J} [C(\nu_j)\tilde{g}_1(\nu_j)\exp(-cz/\nu_j) + C(-\nu_j)\tilde{g}_1(-\nu_j)\exp(cz/\nu_j)], \quad \text{(A2)}$$

where $C(\pm\nu_j)$ are expansion coefficients, ν_j are the J eigenvalues of Eq. (1) corresponding to the eigenfunctions[23] $\phi(\pm\nu_j,\mu)$, and

$$\tilde{g}_j(\pm\nu_1) = \int_0^1 \phi(\pm\nu_j,\mu)P_j(\mu)d\mu \quad \text{(A3)}$$

for Legendre polynomial $P_j(\mu)$. Far from the boundaries, $E_d(z)$ and $L_u(z)$ can be approximated by retaining only the asymptotic decreasing eigenmode corresponding to the largest eigenvalue ν_1 [i.e., $C(\nu_j) = 0$ for $j > 1$ and $C(-\nu_j) = 0$ for all j], and since $R^L(z) = \pi L_u(z)/E_d(z)$ the asymptotic value of $R^L(z)$ is $R^L_\infty = \pi\phi(\nu_1,-1)/\tilde{g}_1(\nu_1)$. At depths far from the surface but where some influence of the bottom is present, $E_d(z)$ and $L_u(z)$ are better approximated by also including the eigenmode corresponding to the largest negative eigenvalue, $-\nu_1$, so then

$$L_u(z) \approx C(\nu_1)\phi(\nu_1,-1)\exp(-cz/\nu_1) + C(-\nu_1)\phi(-\nu_1,-1)\exp(cz/\nu_1), \quad \text{(A4)}$$

$$E_d(z) \approx C(\nu_1)\tilde{g}_1(\nu_1)\exp(-cz/\nu_1) + C(-\nu_1)\tilde{g}_1(-\nu_1)\exp(cz/\nu_1). \quad \text{(A5)}$$

After forming the ratio $R^L(z) = \pi L_u(z)/E_d(z)$, dividing through by $C(\nu_1)\tilde{g}_1(\nu_1)\exp(-cz/\nu_1)$, letting $r = C(-\nu_1)/C(\nu_1)$, and recognizing that[13] $R^L_\infty = \phi(-\nu_1,1)/\tilde{g}_1(\nu_1)$, we find that

$$R^L(z) = \frac{R^L_\infty + \pi r\phi(-\nu_1,-1)\exp(2cz/\nu_1)/\tilde{g}_1(\nu_1)}{1 + rR_\infty\exp(2cz/\nu_1)}. \quad \text{(A6)}$$

Subtraction of R^L_∞ from Eq. (A6) gives,

$$R^L(z) - R^L_\infty = \frac{r\exp(2cz/\nu_1)[\pi\phi(-\nu_1,-1)/\tilde{g}_1(\nu_1) - R^L_\infty R_\infty]}{1 + rR_\infty\exp(2cz/\nu_1)}. \quad \text{(A7)}$$

A rearrangement of this equation is,

$$[R^L(z) - R^L_\infty] \exp(-2cz/\nu_1)[1 + rR_\infty \exp(2cz/\nu_1)] = r[\pi\phi(-\nu_1, -1)/\tilde{g}_1(\nu_1) - R^L_\infty R_\infty]. \quad \text{(A8)}$$

Since the RHS of Eq. (A8) is independent of z, the LHS at arbitrary depth z equals that at the bottom. Therefore,

$$R^L(z) = R^L_\infty + [R^L(z_b) - R^L_\infty] \exp[-2c(z_b - z)/\nu_1] \left[\frac{1 + rR_\infty \exp(2cz_b/\nu_1)}{1 + rR_\infty \exp(2cz/\nu_1)}\right]. \quad \text{(A9)}$$

If $[rR_\infty \exp(2cz_b/\nu_1)] \ll 1$ or if $(z_b - z)$ is small, then Eq. (A9) reduces to

$$R^L(z) = R^L_\infty + [R^L(z_b) - R^L_\infty] \exp[-2c(z_b - z)/\nu_1], \quad \text{(A10)}$$

which is analogous to our equation for $R(z)$ derived in a similar manner.[17] Rearrangement of Eq. (A10) gives Eq. (10).

REFERENCES

1. S. G. Ackleson, "Diffuse attenuation in optically-shallow water: effects of bottom reflectance," in *Ocean Optics XIII*, S. G. Ackleson and R. Frouin, eds., Proc. Soc. Photo-Opt. Instrum. Eng. **2963**, 326–330 (1997).

2. C. D. Mobley, *Light and Water. Radiative Transfer in Natural Waters* (Academic Press, New York, 1994).

3. H. R. Gordon and O. B. Brown, "Influence of bottom depth and albedo on reflectance of a flat homogeneous ocean," Appl. Opt. **13**, 2153–2159 (1974).

4. S. Maritorena, A. Morel, and B. Gentili, "Diffuse reflectance of oceanic shallow waters: Influence of water depth and bottom albedo," Limnol. Oceanogr. **39**, 1689–1703 (1994).

5. D. R. Lyzenga, "Passive remote sensing techniques for mapping water depth and bottom features," Appl. Opt. **17**, 379–383 (1978).

6. R. W. Gould, Jr. and R. A. Arnone, "Remote sensing estimates of inherent optical properties in a coastal environment," Int. J. Remote Sensing **61**, 290–301 (1997).

7. Z. Lee, K. L. Carder, S. K. Hawes, R. G. Steward, T. G. Peacock, and C. O. Davis, "Model for the interpretation of hyperspectral remote-sensing reflectance," Appl. Opt. **33**, 5721–5732 (1994).

8. P. Pratt, K. L. Carder, D. K. Costello, and Z. Lee, "Algorithms for path radiance and attenuation to provide color-corrections for underwater imagery, characterize optical properties and determine bottom albedo," in *Ocean Optics XIII*, S. G. Ackleson and R. Frouin, eds., Proc. Soc. Photo-Opt. Instrum. Eng. **2963**, 753–759 (1997).

9. E. LeDrew, H. Holden, D. Peddle, and J. Morrow, "Mapping coral ecosystems in Fiji from SPOT imagery with in situ optical correction," in *Information tools for sustainable*

development, Proc. 26th Int. Symp. Remote Sensing Environ. and 18th Symp. Can. Remote Sensing Soc., Canadian Aeronautic and Space Inst., Ottawa, Ontario, 581–584 (1996).

10. G. N. Plass and G. W. Kattawar, "Monte Carlo calculations of radiative transfer in the earth's atmosphere-ocean system: I. Flux in the atmosphere and ocean," J. Phys. Ocean., **2**, 139–145 (1972).

11. S. Maritorena, "Remote sensing of the water attenuation in coral reefs: a case study in French Polynesia," Int. J. Remote Sensing **17**, 155–166 (1996).

12. D. R. Lyzenga, "Remote sensing of bottom reflectance and water attenuation parameters in shallow water using aircraft and Landsat data," Int. J. Remote Sensing **2**, 71–82 (1981).

13. N. J. McCormick, "Analytical transport theory applications in optical oceanography," Ann. Nucl. Energy **23**, 381–395 (1996).

14. W. D. Philpot, "Radiative transfer in stratified waters: a single-scattering approximation for irradiance," Appl. Opt. **26**, 4123–4132 (1987).

15. J. T. O. Kirk, "The upwelling light stream in natural waters," Limnol. Oceanogr. **34**, 1410–1425 (1989).

16. N. T. O'Neill and J. R. Miller, "On calibration of passive optical bathymetry from the spatial variation of environmental parameters," Int. J. Remote Sensing **10**, 1481–1501 (1989).

17. R. A. Leathers and N. J. McCormick, "Ocean inherent optical property estimation from irradiances," Appl. Opt. **36**, 8685–8698 (1997).

18. M. Kishino, "Interrelationship between light and phytoplankton in the sea," in *Ocean*

Optics, R. W. Spinrad, K. L. Carder, and M. J. Perry, eds. (Oxford U. Press, New York, 1994).

19. J. R. V. Zaneveld, "A reflecting tube absorption meter," in *Ocean Optics X*, R. W. Spinrad, ed., Proc. Soc. Photo-Opt. Instrum. Eng. **1302**, 124–136 (1990).

20. Z. Jin and K. Stamnes, "Radiative transfer in nonuniformly refracting layered media such as the atmosphere/ocean system," Appl. Opt. **33**, 431–442 (1994).

21. C. D. Mobley, B. Gentili, H. R. Gordon, Z. Jin, G. W. Kattawar, A. Morel, P. Reinersman, K. Stamnes, and R. H. Stavn, "Comparison of numerical models for computing underwater light fields," Appl. Opt., **32**, 7484–7504 (1993).

22. C. D. Mobley, Sequoia Scientific, Inc. (Mercer Island, WA), private communication (1999).

23. N. J. McCormick, "Asymptotic optical attenuation," Limnol. Oceanogr. **37**, 1570–1578 (1992).

FIGURES

Fig. 1. Profiles of estimates of the bottom albedo, $\widehat{R_b}(\tau)$, with a) the estimate equal to the irradiance reflectance, $R(\tau)$, b) Eq. (8) with known R_∞ and K_∞, and c) Eqs. (8) and (9). The simulation was generated for $R_b = 0.2$, five optical depth water, $\omega_0 = 0.8$, and 75% collimated light at 30° from the zenith.

Fig. 2. Profiles of estimates of the bottom albedo, $\widehat{R_b}(\tau)$, with the two-site E_u–E_d method of Eq. (7) for (left) $\omega_0 = 0.7$ and $R_b = 0.2$ and for (right) $\omega_0 = 0.9$ and $R_b = 0.1$. The simulations were for sunny conditions, and the R_b determination was done with K in Eq. (7) replaced by $\overline{K_d(z)}$ (*) and by the deep (asymptotic) value of $K_d(z)$ (–).

Fig. 3. Profiles of estimates of the bottom albedo, $\widehat{R_b}(\tau)$, from $E_u(z)$ and $E_d(z)$ with the two-site method of Eq. (7) (*) and the one site method of Eq. (8) (–). These sunny sky simulations were for (left) $\omega_0 = 0.9$ and $R_b = 0.1$ and for (right) $\omega_0 = 0.8$ and $R_b = 0.2$.

Fig. 4. Profiles of estimates of the bottom albedo, $\widehat{R_b}(\tau)$, from $L_u(z)$ and $E_d(z)$ with the two-site method of Eq. (11) (*) and the one site method of Eq. (10) (–). The simulations were for (left) sunny conditions, $\omega_0 = 0.9$ and $R_b = 0.1$ and for (right) overcast conditions, $\omega_0 = 0.9$ and $R_b = 0.2$.

TABLES

Table 1. Calculations of the bottom albedo with Eqs. (8) and (9) from simulated irradiance measurements at three, two, and one optical depths above the bottom and extrapolations to the bottom of the latter two.

simulation				$\widehat{R_b}(\tau)$			
ω_0	τ_b	R_b	illumination	$\tau_b - 3$	$\tau_b - 2$	$\tau_b - 1$	extrapolation
0.7	3	0.2	sunny	N/A	0.177	0.189	0.200
0.7	5	0.1	sunny	0.091	0.091	0.096	0.101
0.7	5	0.2	sunny	0.170	0.176	0.189	0.202
0.7	5	0.2	overcast	0.172	0.177	0.190	0.202
0.7	7	0.2	sunny	0.167	0.176	0.189	0.203
0.8	5	0.2	sunny	0.186	0.188	0.194	0.201
0.9	5	0.1	sunny	0.114	0.106	0.102	0.098
0.9	5	0.2	sunny	0.207	0.201	0.200	0.199
0.9	5	0.2	overcast	0.207	0.201	0.200	0.199
0.9	5	0.3	sunny	0.296	0.294	0.297	0.300
0.9	5	0.4	sunny	0.385	0.387	0.395	0.403

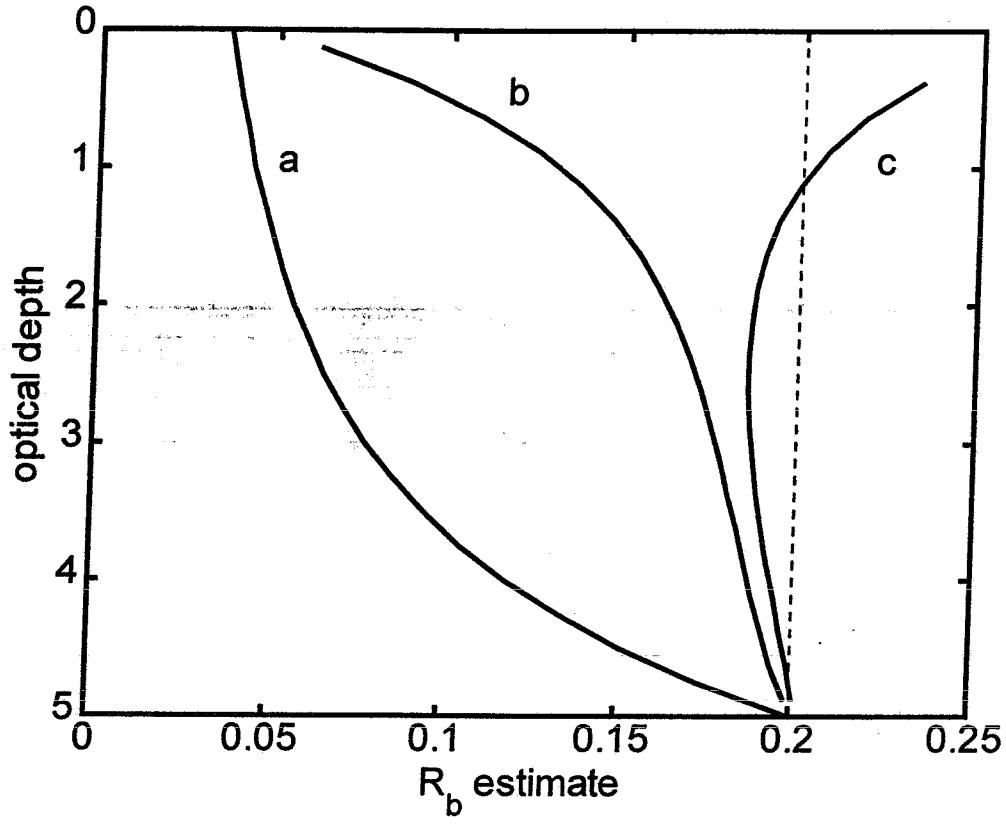

Fig. 1. Profiles of estimates of the bottom albedo, $\widehat{R_b}(\tau)$, with a) the estimate equal to the irradiance reflectance, $R(\tau)$, b) Eq. (8) with known R_∞ and K_∞, and c) Eqs. (8) and (9). The simulation was generated for $R_b = 0.2$, five optical depth water, $\omega_0 = 0.8$, and 75% collimated light at 30° from the zenith.

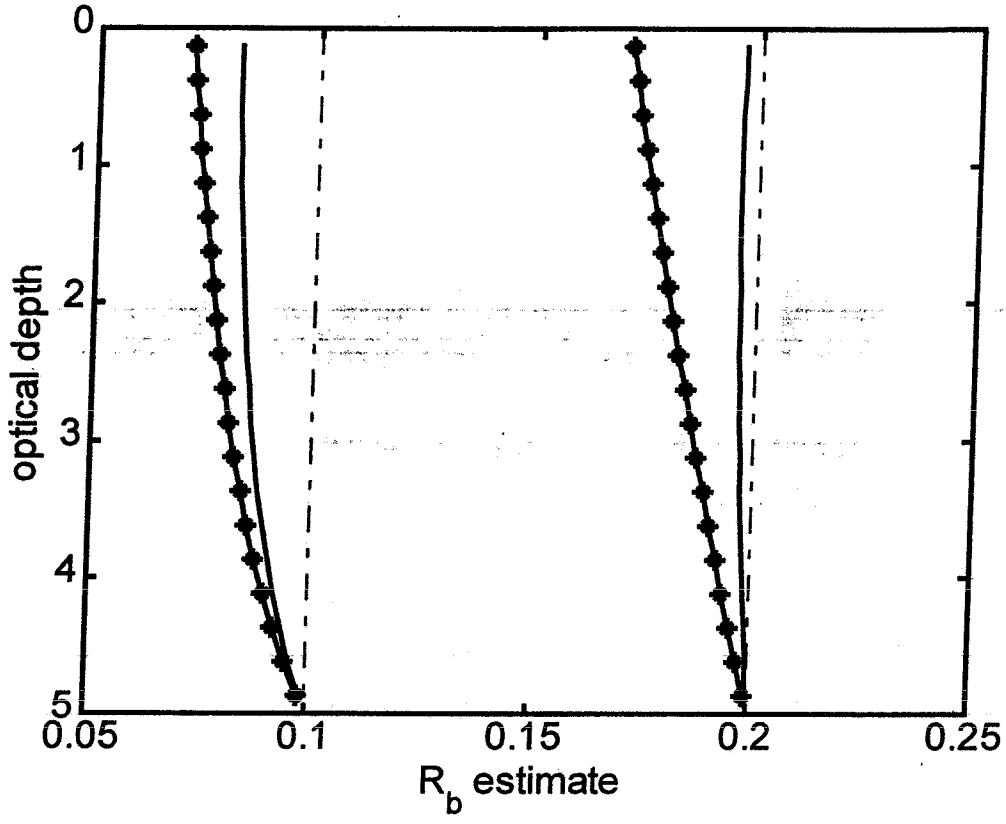

Fig. 2. Profiles of estimates of the bottom albedo, $\widehat{R_b}(\tau)$, with the two-site E_u–E_d method of Eq. (7) for (left) $\omega_0 = 0.7$ and $R_b = 0.2$ and for (right) $\omega_0 = 0.9$ and $R_b = 0.1$. The simulations were for sunny conditions, and the R_b determination was done with K in Eq. (7) replaced by $\overline{K_d(z)}$ (*) and by the deep (asymptotic) value of $K_d(z)$ (–).

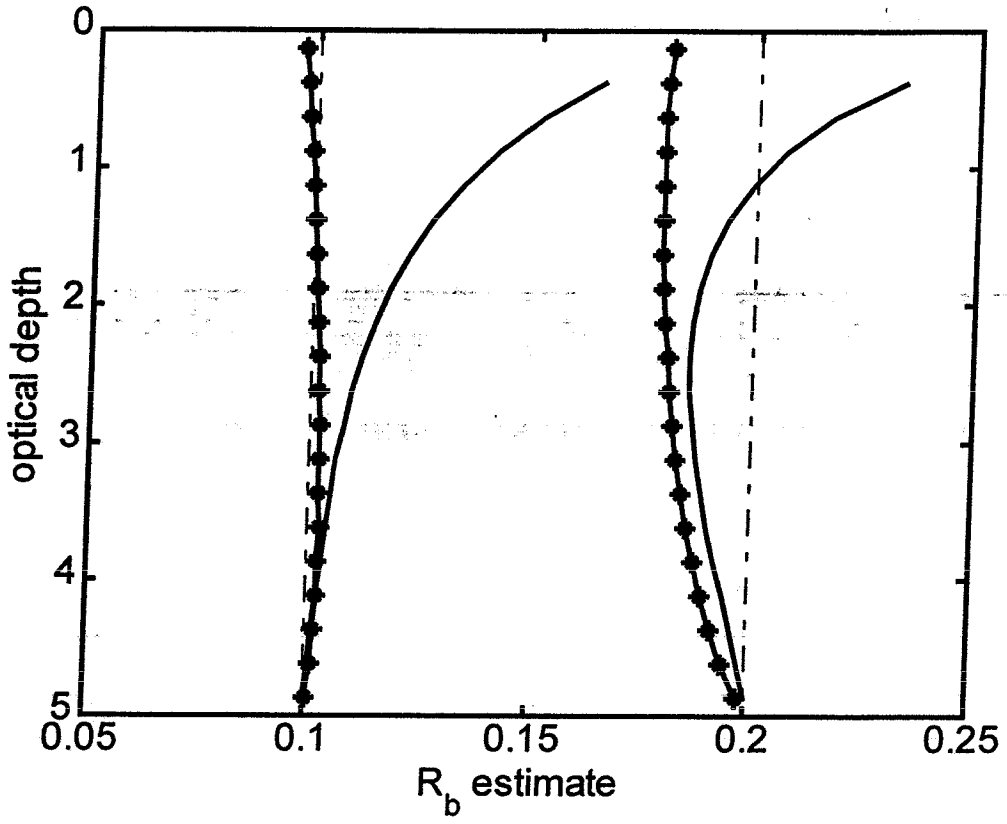

Fig. 3. Profiles of estimates of the bottom albedo, $\widehat{R_b}(\tau)$, from $E_u(z)$ and $E_d(z)$ with the two-site method of Eq. (7) (*) and the one site method of Eq. (8) (–). These sunny sky simulations were for (left) $\omega_0 = 0.9$ and $R_b = 0.1$ and for (right) $\omega_0 = 0.8$ and $R_b = 0.2$.

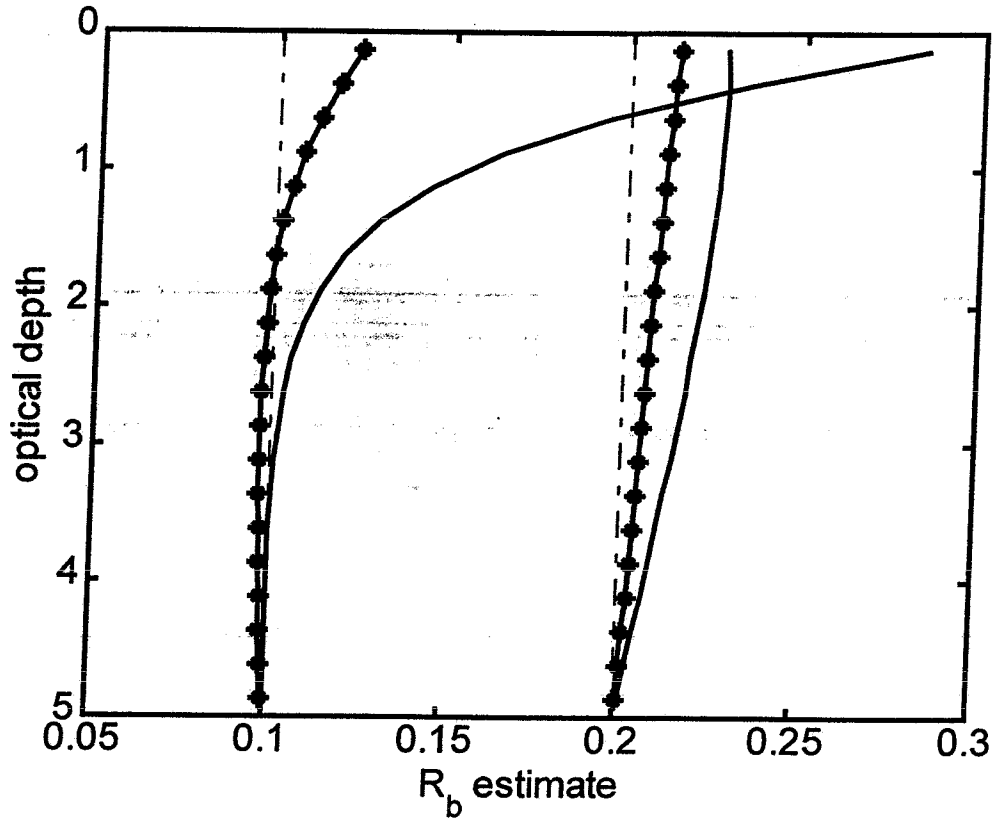

Fig. 4. Profiles of estimates of the bottom albedo, $\widehat{R_b}(\tau)$, from $L_u(z)$ and $E_d(z)$ with the two-site method of Eq. (11) (*) and the one site method of Eq. (10) (–). The simulations were for (left) sunny conditions, $\omega_0 = 0.9$ and $R_b = 0.1$ and for (right) overcast conditions, $\omega_0 = 0.9$ and $R_b = 0.2$.

REPORT DOCUMENTION PAGE

Form Approved
OMB No. 0704-0188

1. AGENCY USE ONLY *(Leave blank)*	2. REPORT DATE	3. REPORT TYPE AND DATES COVERED
	1999	final

4. TITLE AND SUBTITLE

Algorithms for ocean bottom albedo determination from in-water natural light measurements

5. FUNDING NUMBERS

6. AUTHOR(S)

Robert A. Leathers and Norman J. McCormick

7. PERFORMING ORGANIZATION NAME(S) AND ADDRESS(ES)

ESSO/SSC

8. PERFORMING ORGANIZATION REPORT NUMBER

9. SPONSORING/MONITORING AGENCY NAME(S) AND ADDRESS(ES)

NASA/SSC

10. SPONSORING/MONITORING AGENCY REPORT NUMBER

11. SUPPLEMENTARY NOTES

To be published in Applied Optics

12a. DISTRIBUTION/AVAILABILITY STATEMENT

Publicly Available

12b. DISTRIBUTION CODE

13. ABSTRACT ***(Maximum 200 words)***

A method for determining the ocean bottom optical albedo, Rb, from in-water upward and downward irradiance measurements at a shallow site is presented, tested, and compared with a more familiar approach that requires additional measurements at a nearby deep-water site. Also presented are two new algorithms for the estimation of Rb from measurements of the downward irradiance and vertically upward radiance. All methods performed well in numerical situations at depths where the influence of the bottom on the light field was significant.

14. SUBJECT TERMS

Ocean optics, radiative transfer, inverse problem, bottom albedo

15. NUMBER OF PAGES

4

16. PRICE CODE

17. SECURITY CLASSIFICATION OF REPORT	18. SECURITY CLASSIFICATION OF THIS PAGE	19. SECURITY CLASSIFICATION OF ABSTRACT	20. LIMITATION OF ABSTRACT
Unclassified	Unclassified	Unclassified	UL